Available online at www.sciencedirect.com
ScienceDirect
International Journal of Thermal Sciences 47 (2008) 1374–1381
International Journal of Thermal Sciences
www.elsevier.com/locate/ijts

Influence of multi-irreversibilities on the performance of a Brayton refrigeration cycle working with an ideal Bose or Fermi gas

Jingyi Liu [a,b], Bihong Lin [a,c], Weiqiang Hu [a], Jincan Chen [a,*]

[a] *Department of Physics, Xiamen University, Xiamen 361005, People's Republic of China*
[b] *Department of Physics and Electric Information Engineering, Zhangzhou normal University, Zhangzhou 363000, People's Republic of China*
[c] *Department of Physics, Quanzhou normal University, Quanzhou 362000, People's Republic of China*

Received 31 March 2007; received in revised form 21 October 2007; accepted 22 October 2007

Available online 20 February 2008

Abstract

An irreversible cycle model of the quantum Brayton refrigeration cycle using an ideal Bose or Fermi gas as the working substance is established. Based on the theory of statistical mechanics and thermodynamic properties of ideal quantum gases, expressions for several important performance parameters such as the cooling rate, coefficient of performance and power input, are derived. The influence of the degeneracy of quantum gases, the internal irreversibility of the working substance and the finite-rate heat transfer between the working substance and the heat reservoirs on the optimal performance of the cycle is investigated. By using numerical solutions, the cooling rate of the cycle is optimized for a set of given parameters. The maximum cooling rate and the corresponding parameters are calculated numerically. The optimal boundaries of the coefficient of performance and power input are given. The optimally operating region of the cycle is determined. The expressions of some performance parameters for some special cases are derived analytically.

Keywords: Brayton refrigeration cycle; Quantum gas; Irreversibility; Performance parameter; Optimal analysis

1. Introduction

For a cryogenic refrigeration device, the performance of the working substance can be only described by the theory of quantum statistical mechanics instead of that of classical statistical mechanics. The influence of the quantum characteristics of the working substance on the performance of the cycle must be considered in thermodynamic analysis [1–7]. In recent years, the performance analysis of the cryogenic thermodynamic cycles, which may be called the quantum thermodynamic cycles, has become one of the interesting research subjects on thermodynamics and statistical physics. Many authors have studied the performance characteristics of the cryogenic refrigeration cycles working with ideal quantum gases based on the statistical mechanics and thermodynamic theory [7–15]. Many meaningful conclusions have been obtained.

It is well known that the previous investigation on the quantum thermodynamic cycles mainly focuses on the effects of the quantum degeneracy [1–4,8,10,13,14], regeneration [9,15] and irreversibility [5,11,12] on the performance of the thermodynamic cycles working with quantum gases. For example, Saygin and Sisman [1–3,8], He et al. [10], and Lin et al. [13,14] analyzed the influence of the quantum degeneracy on the performance of the quantum thermodynamic cycle working with ideal quantum gases. Chen et al. [9] and Yang et al. [15] investigated the influence of the regeneration on the performance of the quantum thermodynamic cycle working with ideal quantum gases. Wu et al. [5,12] and Zhang et al. [11] researched the effect of irreversibility on the optimal performance of the irreversible quantum Brayton cycles with ideal quantum gases. Recently, the influence of the irreversibility of finite-rate heat transfer between the working substance and the heat reservoirs on the cooling rate and the optimal performance of an irreversible cryogenic refrigeration cycle using an ideal quantum gas as the refrigerant has been also considered [7]. However, the influence of the irreversibility of finite-rate heat transfer

* Corresponding author.
E-mail address: jcchen@xmu.edu.cn (J. Chen).

1290-0729/$ – see front matter
doi:10.1016/j.ijthermalsci.2007.10.013

Nomenclature

A	total heat transfer area	m^2	
A_H	heat transfer area between the working substance and the heat sink	m^2	
A_L	heat transfer area between the working substance and the cooled space	m^2	
C_P	heat capacity at constant-pressure	$J K^{-1}$	
$F(z)$	correction function		
h	Planck constant	J s	
k	Boltzmann constant	$J K^{-1}$	
m	rest mass of a particle	kg	
P_H	pressure of high constant-pressure process	Pa	
P_L	pressure of low constant-pressure process	Pa	
Q_H	amount of heat released to the heat sink	J	
Q_L	refrigeration load	J	
r_P	pressure ratio		
R	cooling rate	W	
$R_{\max}$	maximum cooling rate	W	
T_i	temperature at state i	K	
T_H	temperature of the heat sink	K	
T_L	temperature of the cooled space	K	
U_H	heat transfer coefficient between the working substance and the heat sink	$J K^{-1} s^{-1}$	
U_L	heat transfer coefficient between the working substance and the cooled space	$J K^{-1} s^{-1}$	
$\dot{W}$	power input	W	
$\dot{W}_m$	power input at the maximum cooling rate	W	
z	fugacity		

Greek symbols

ε	coefficient of performance	
ε_m	coefficient of performance at the maximum cooling rate	
η_c	compression efficiencies	
η_e	expansion efficiencies	
τ	cycle period	s

on the performance of a quantum Brayton refrigeration cycle has been rarely studied. Consequently, it is of significance to investigate the synthesis influence of the various irreversibilities, which especially include the finite-rate heat transfer, on the optimal performance of the quantum Brayton cryogenic refrigeration cycle.

In the present paper, the optimal performance characteristics of the irreversible Brayton cryogenic refrigeration cycle composed of two adiabatic and two isobaric processes are investigated. The working substance of the cycle consists of ideal Fermi or Bose gases. The general expressions of several important parameters such as the cooling rate, power input and coefficient of performance are derived. The performance characteristics of the cycle are revealed. The curves of the optimal relation between the cooling rate and the coefficient of performance are obtained. The optimal performances of the cycle are discussed in detail. The optimum criteria of some important parameters are obtained.

2. An irreversible Brayton refrigeration cycle

An irreversible Brayton refrigeration cycle using an ideal Bose or Fermi gas as the working substance may be simply called the irreversible quantum Brayton refrigeration cycle. It is composed of two adiabatic and two constant-pressure processes and operated between the heat sink at temperature T_H and the cooled space at temperature T_L. The temperature–entropy diagram of the cycle is shown in Fig. 1, where the two dashed lines indicate two irreversible adiabatic processes (2-3 and 4-1), the two vertical solid lines indicate two reversible adiabatic processes (2-3S and 4-1S), P_H and P_L are the pressures of the high and low constant-pressure processes, Q_H and Q_L are the amounts of heat exchanged between the working substance and the heat reservoirs in the two constant-pressure processes per cycle, and the temperatures at state points 1S, 1, 2, 3, 3S and 4

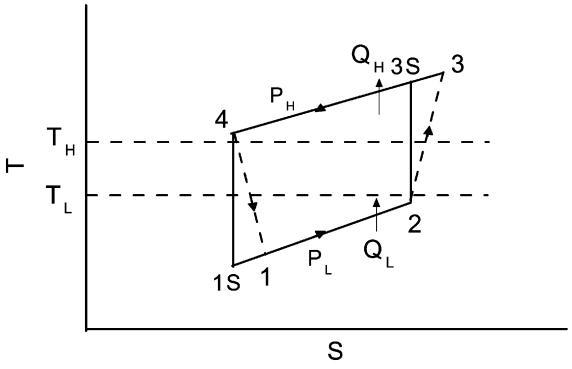

Fig. 1. The T–S diagram of an irreversible quantum Brayton refrigeration cycle.

are indicated by T_{1S}, T_1, T_2, T_3, T_{3S} and T_4, respectively. In a real refrigerator, owing to the internal dissipation of the working substance, all the processes are irreversible. According to Fig. 1, one may introduce the compression and expansion efficiencies [16–27]

$$\eta_c = \frac{T_{3S} - T_2}{T_3 - T_2} \tag{1}$$

and

$$\eta_e = \frac{T_4 - T_1}{T_4 - T_{1S}} \tag{2}$$

to describe the irreversibility of the adiabatic processes. When $\eta_c = 1$ and $\eta_e = 1$, the adiabatic compression and expansion processes become reversible.

According to quantum statistical mechanics [28,29] and the thermodynamic properties of ideal Fermi and Bose gases, one can calculate that the amounts of heat exchanged between the

working substance and the heat reservoirs in the two isobaric processes of the cycle are, respectively, given by [11]

$$Q_L = \int_{T_1}^{T_2} C_P \,\mathrm{d}T = \frac{5}{2}Nk\big[T_2F(T_2, P_L) - T_1F(T_1, P_L)\big] \tag{3}$$

and

$$Q_H = \int_{T_4}^{T_3} C_P \,\mathrm{d}T = \frac{5}{2}Nk\big[T_3F(T_3, P_H) - T_4F(T_4, P_H)\big] \tag{4}$$

where $C_P = \frac{5}{2}Nk\{\frac{\partial}{\partial T}[TF(T, P)]\}_P$ is the heat capacity at constant-pressure, k is the Boltzmann constant,

$$F(T, P) = F(z) = \left[\frac{1}{\Gamma(5/2)}\int_0^\infty \frac{x^{3/2}}{z^{-1}\mathrm{e}^x \pm 1}\,\mathrm{d}x\right] \times \left[\frac{1}{\Gamma(3/2)}\int_0^\infty \frac{x^{1/2}}{z^{-1}\mathrm{e}^x \pm 1}\,\mathrm{d}x\right]^{-1}$$

is the correction function, $f_l(z) = \frac{1}{\Gamma(l)}\int_0^\infty \frac{x^{l-1}}{z^{-1}\mathrm{e}^x+1}\,\mathrm{d}x$ is called the Fermi integral, $g_l(z) = \frac{1}{\Gamma(l)}\int_0^\infty \frac{x^{l-1}}{z^{-1}\mathrm{e}^x-1}\,\mathrm{d}x$ is called the Bose integral, z is the fugacity, $\Gamma(5/2) = 1.32934$, $\Gamma(3/2) = 0.886227$, and the sign "±" correspond to ideal Fermi and Bose gases, respectively. When the two adiabatic processes are reversible, one can obtain [13]

$$\frac{T_{3S}}{T_2} = \frac{T_4}{T_{1S}} = \left(\frac{P_H}{P_L}\right)^{2/5} = r_P^{2/5} \tag{5}$$

where $r_P = P_H/P_L$ is the ratio of the pressures in the high and low constant-pressure processes.

From Eqs. (1), (2) and (5), one can obtain

$$T_1 = \big[1 - \eta_e\big(1 - r_P^{-2/5}\big)\big]T_4 = XT_4 \tag{6}$$

and

$$T_3 = \big[1 + \eta_c^{-1}\big(r_P^{2/5} - 1\big)\big]T_2 = YT_2 \tag{7}$$

where $X = 1 - \eta_e(1 - r_P^{-2/5})$ and $Y = 1 + \eta_c^{-1}(r_P^{2/5} - 1)$. By using Eqs. (6) and (7), Eqs. (3) and (4) can be further expressed as

$$Q_L = \int_{T_1}^{T_2} C_P \,\mathrm{d}T = \frac{5}{2}Nk\big[T_2F(T_2, P_L) - XT_4F(XT_4, P_L)\big] \tag{8}$$

and

$$Q_H = \int_{T_4}^{T_3} C_P \,\mathrm{d}T = \frac{5}{2}Nk\big[YT_2F(YT_2, P_H) - T_4F(T_4, P_H)\big] \tag{9}$$

When heat transfer obeys Newton's heat transfer law [30,31], Q_L and Q_H can be, respectively, expressed as

$$Q_L = U_LA_L(T_2 - T_1)\tau/\ln\big[(T_L - T_1)/(T_L - T_2)\big] \tag{10}$$

and

$$Q_H = U_HA_H(T_3 - T_4)\tau/\ln\big[(T_3 - T_H)/(T_4 - T_H)\big] \tag{11}$$

where U_L and U_H are, respectively, the heat transfer coefficients between the refrigerator and the reservoirs, A_L and A_H are, respectively, the heat transfer areas between the refrigerator and the reservoirs, and τ is the cycle period. The total heat transfer area A of the cycle is

$$A = A_L + A_H \tag{12}$$

Using Eqs. (6)–(12), one can obtain the expressions of the ratios of the cold-side and hot-side heat transfer areas to the total heat transfer area as

$$A_L = \frac{A}{1 + B\frac{U_L(T_2 - XT_4)\ln[(YT_2 - T_H)/(T_4 - T_H)]}{U_H(YT_2 - T_4)\ln[(T_L - XT_4)/(T_L - T_2)]}} \tag{13}$$

and

$$A_H = \frac{A}{1 + \frac{1}{B}\frac{U_H(YT_2 - T_4)\ln[(T_L - XT_4)/(T_L - T_2)]}{U_L(T_2 - XT_4)\ln[(YT_2 - T_H)/(T_4 - T_H)]}} \tag{14}$$

where $B = \frac{YT_2F(YT_2, P_H) - T_4F(T_4, P_H)}{T_2F(T_2, P_L) - XT_4F(XT_4, P_L)}$.

3. Expressions of several important parameters

The cooling rate, coefficient of performance and power input are three important parameters of a quantum Brayton refrigeration cycle. In order to understand the performance of a quantum Brayton refrigeration cycle, one must derive the expressions of these three parameters. Using Eqs. (8)–(11), (13) and (14), we find that the cooling rate, coefficient of performance and power input may be, respectively, expressed as

$$R = \frac{Q_L}{\tau} = \big\{AU_HU_L(YT_2 - T_4)(T_2 - XT_4)\big\} / \big\{U_H(YT_2 - T_4)\ln\big[(T_L - XT_4)/(T_L - T_2)\big] + U_LB(T_2 - XT_4)\ln\big[(YT_2 - T_H)/(T_4 - T_H)\big]\big\} \tag{15}$$

$$\varepsilon = \frac{Q_L}{Q_H - Q_L} = \frac{1}{B - 1} \tag{16}$$

and

$$\dot{W} = \frac{Q_H - Q_L}{\tau} = \big\{U_HU_LA(YT_2 - T_4)(T_2 - XT_4)(B - 1)\big\} / \big\{U_H(YT_2 - T_4)\ln\big[(T_L - XT_4)/(T_L - T_2)\big] + U_LB(T_2 - XT_4)\ln\big[(YT_2 - T_H)/(T_4 - T_H)\big]\big\} \tag{17}$$

Using the above equations, one can analyze the general performance characteristics of an irreversible quantum Brayton refrigeration cycle and give the optimal criteria of some important performance parameters.

4. General optimum performance characteristics

It is seen from Eq. (15) that the cooling rate is a function of two variables (T_2, T_4) for given values of the other parameters. Choosing ^{4}He and ^{3}He gas as the working substance of the cycle and using Eq. (15) and the thermodynamic properties of ideal Bose and Fermi gases, one can generate three-dimensional graphs (T_2, T_4, R^*), as shown in Fig. 2(a) and (b), respectively, where $R^* = R/(AUT_L)$ is the dimensionless cooling rate and the parameters $T_L = 10$ K, $T_H = 25$ K, $P_L = 0.6$ MPa, $r_P = 50$, $\eta_e = \eta_c = 0.95$ and $U_L = U_H = U$ are chosen [32–35]. It can be seen from Fig. 2 that the cooling rate R first increases and then decreases as T_2 or T_4 increases. It shows clearly that there are the optimal values of T_2 and T_4 at which the cooling rate R attains its maximum for a set of given values of the other parameters. One can solve Eqs. (13)–(17) numerically and generate the $R^*_{\max} \sim r_P$, $\varepsilon_m \sim r_P$, $R^* \sim \varepsilon$, $\dot{W}^* \sim \varepsilon$, $T_{im} \sim r_P$ $(i = 1, 2, 3, 4)$, $(A_L/A)_m \sim r_P$ and $(A_H/A)_m \sim r_P$ optimal characteristic curves of the cycle, as shown in Figs. 3–8, respectively, where $\dot{W}^* = \dot{W}/(AUT_L)$ is the dimensionless power input, and ε_m, T_{im} $(i = 1, 2, 3, 4)$, $(A_L/A)_m$ and $(A_H/A)_m$ are, respectively, the corresponding coefficient of performance, temperatures at state points 1, 2, 3, 4, the ratios of the cold-side and hot-side heat transfer areas to the total heat transfer area at the maximum cooling rate.

It is clearly seen from Figs. 3 and 4 that the maximum cooling rate increases while the corresponding coefficient of performance decreases as the pressure ratio increases. The larger the irreversibility of the adiabatic processes is, the smaller the maximum cooling rate and the corresponding coefficient of performance.

Fig. 5 shows clearly that the fundamental optimal relation between the cooling rate and the coefficient of performance is not monotonic and there exist a maximum cooling rate $R_{\max}$ and a corresponding coefficient of performance ε_m for the given values of the other parameters T_L, T_H, P_L, r_P, U_L and U_H. Obviously, the maximum cooling rate $R_{\max}$ and the corresponding coefficient of performance ε_m will be different for differently given values of the other parameters. Fig. 5 also shows that when $R < R_{\max}$, there are two different coefficients of performance for a given cooling rate R, where one is smaller than ε_m and the other is larger than ε_m. When $\varepsilon < \varepsilon_m$, the cooling rate will decrease as the coefficient of performance is decreased. It indicates that the region $\varepsilon < \varepsilon_m$ is not optimal. Consequently, the optimal region of the coefficient of performance should be

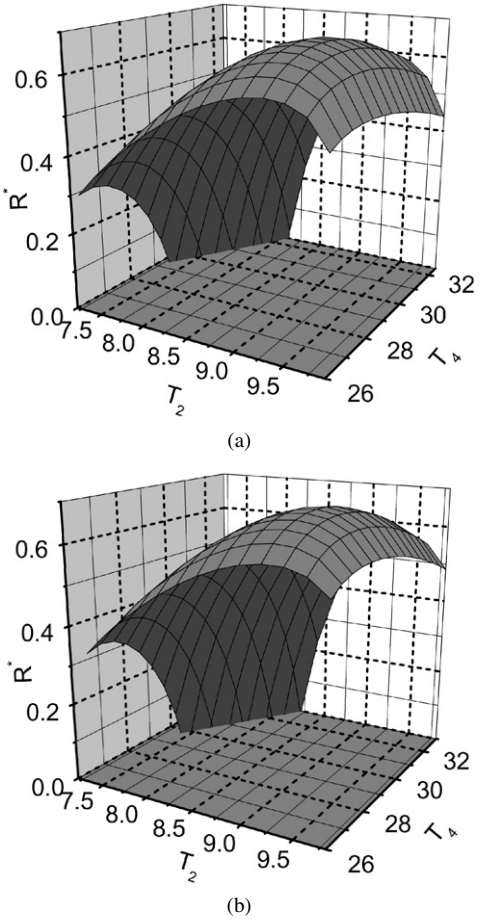

Fig. 2. The cooling rate of the quantum Brayton refrigeration cycle working with the ideal (a) Bose and (b) Fermi gases as a function of the temperatures (T_2, T_4). The graphs are presented for the parameters $T_L = 10$ K, $T_H = 25$ K, $P_L = 0.6$ MPa, $r_P = 50$, $\eta_e = \eta_c = 0.95$ and $U_L = U_H$.

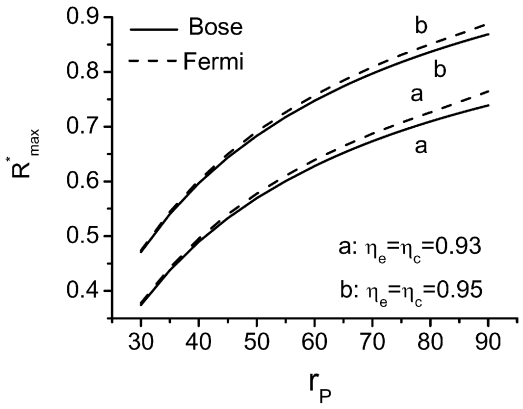

Fig. 3. The $R^*_{\max} \sim r_P$ curves. Curves a and b correspond to the cases of $\eta_e = \eta_c = 0.93$ and $\eta_e = \eta_c = 0.95$, respectively. The values of the other parameters T_H, T_L, U_L, U_H and P_L are the same as those used in Fig. 2.

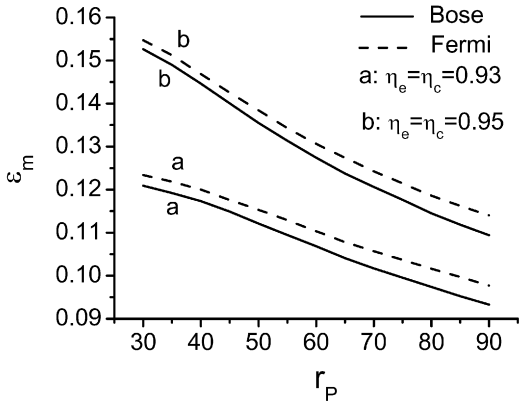

Fig. 4. The $\varepsilon_m \sim r_P$ curves. The values of the parameters $T_H, T_L, U_L, U_H, \eta_c, \eta_e$ and P_L are the same as those used in Fig. 3.

$$\varepsilon \geqslant \varepsilon_m \tag{18}$$

When a quantum Brayton refrigeration cycle is operated in this region, the cooling rate will increase as the coefficient of performance is decreased, and vice versa.

According to Eq. (18), one can further determine the optimal region of the power input as

$$\dot{W} \leqslant \dot{W}_m \tag{19}$$

where W_m is the power input at the maximum cooling rate, as shown in Fig. 6.

The above results show clearly that the maximum cooling rate $R_{\max}$, coefficient of performance ε_m and power input $\dot{W}_m$ at the maximum cooling rate are three important performance parameters of an irreversible quantum Brayton refrigeration cycle, where ε_m and $\dot{W}_m$ determine the allowable values of the

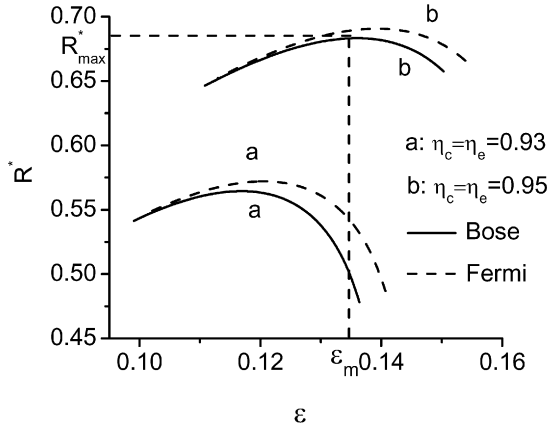

Fig. 5. The $R^* \sim \varepsilon$ curves for $r_P = 50$. The values of the parameters T_H, T_L, U_L, U_H, η_c, η_e and P_L are the same as those used in Fig. 3.

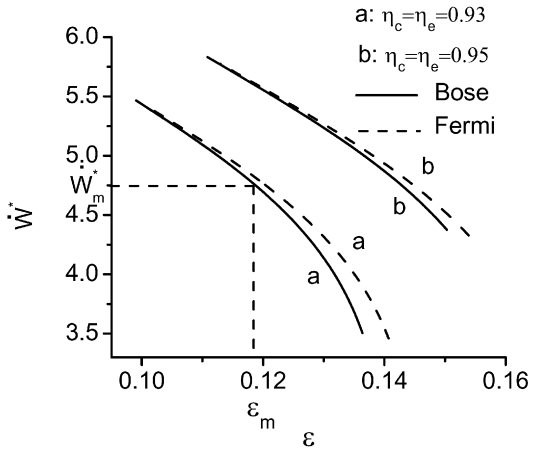

Fig. 6. The $\dot{W}^* \sim \varepsilon$ curves for $r_P = 50$. The values of the parameters T_H, T_L, U_L, U_H, η_c, η_e and P_L are the same as those used in Fig. 3.

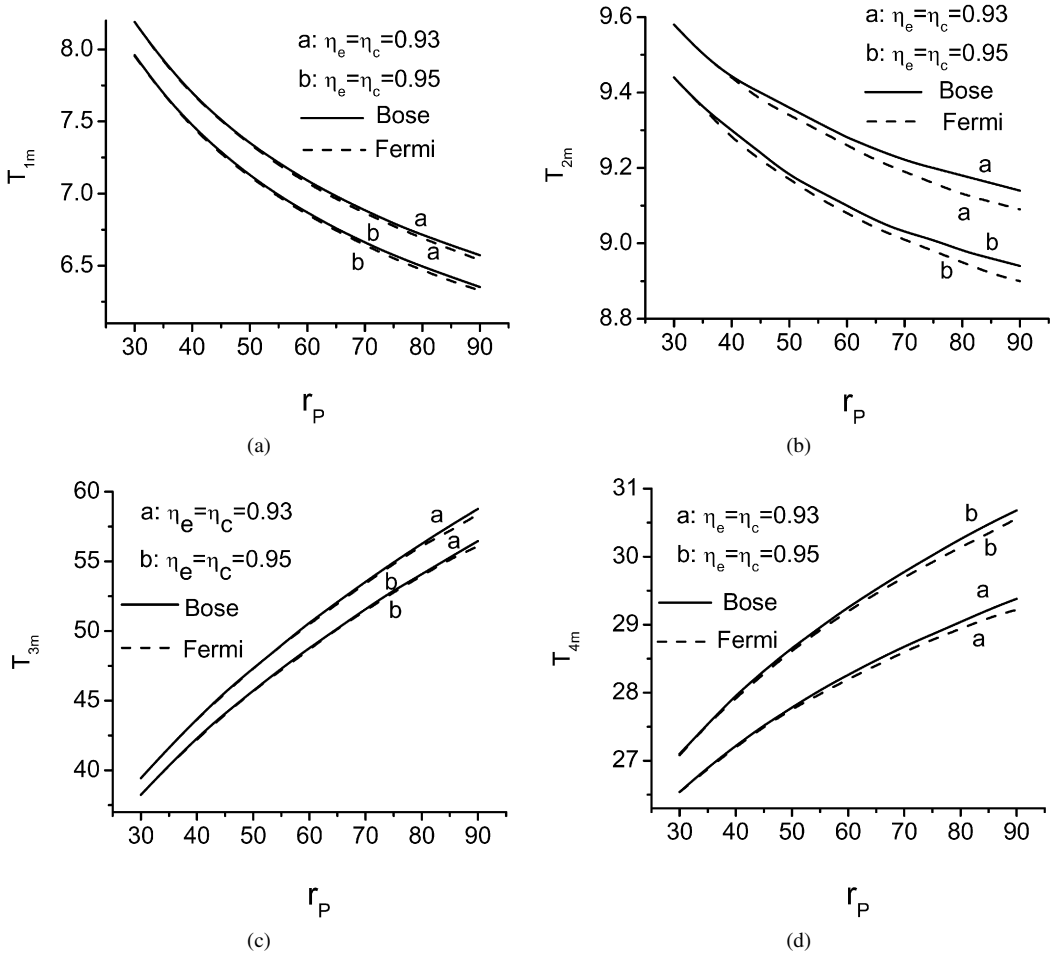

Fig. 7. The $(T_i)_m \sim r_P$ $(i = 1, 2, 3, 4)$ curves. The values of the parameters T_H, T_L, U_L, U_H, η_c, η_e and P_L are the same as those used in Fig. 3.

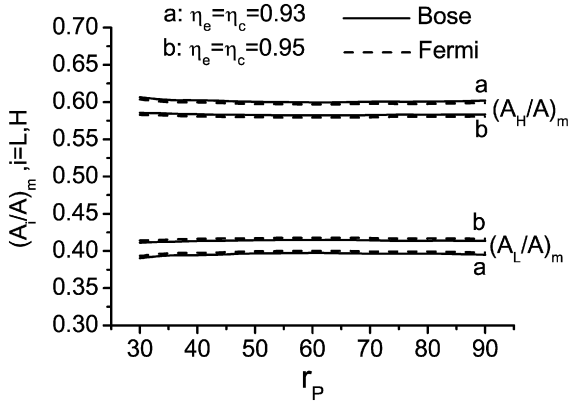

Fig. 8. The $(A_L/A)_m \sim r_P$ and $(A_H/A)_m \sim r_P$ curves. The values of the parameters T_H, T_L, U_L, U_H, η_c, η_e and P_L are the same as those used in Fig. 3.

lower and upper bounds of the optimal coefficient of performance and power input, respectively.

It can be seen from Fig. 7 that the temperatures, T_{1m} and T_{2m}, of the working substance at the maximum cooling rate decrease while T_{3m} and T_{4m} increase as the pressure ratio r_P increases. The larger the irreversibility of the adiabatic processes is, the higher the temperatures T_{1m}, T_{2m} and T_{3m}, while the lower the temperature T_{4m}.

Fig. 8 shows that the influence of the pressure ratio r_P on the ratios of the cold-side and hot-side heat transfer areas to the total heat transfer area at the maximum cooling rate $(A_L/A)_m$ and $(A_H/A)_m$ is small so that $(A_L/A)_m$ and $(A_H/A)_m$ are almost invariable for a large range of r_P. However, the influence of the irreversibility of the adiabatic processes on $(A_L/A)_m$ and $(A_H/A)_m$ is obvious. It is necessary to increase $(A_H/A)_m$ and to decrease $(A_L/A)_m$ as the irreversibility of the adiabatic processes increases.

5. Several interesting cases

It is significant to note that for some special cases, the results obtained above may be simplified.

5.1. Strong gas degeneracy

For an ideal Fermi gas, under the very low-temperature and high-density condition, i.e., the condition of strong gas degeneracy, according to Sommerfeld's lemma, one can derive the first approximation of the correction function as [11]

$$F(T,P)=\frac{2}{5}\frac{DP^{2/5}}{T}+\frac{\pi^2}{10}\frac{T}{DP^{2/5}} \tag{20}$$

where $D=(15\pi^2\hbar^3)^{2/5}/(2km^{3/5})$. By using Eq. (20), Eqs. (15) and (16) may be, respectively, simplified as

$$\begin{aligned}R={}&AU_LU_H\left[T_2^2-(XT_4)^2\right]\\&/\left\{U_H(T_2+XT_4)\ln\left[(T_L-XT_4)/(T_L-T_2)\right]\right.\\&\left.+U_L(YT_2+T_4)r_P^{-2/5}\ln\left[(YT_2-T_H)/(T_4-T_H)\right]\right\}\end{aligned} \tag{21}$$

and

$$\varepsilon=\frac{[T_2^2-(XT_4)^2]}{[(YT_2)^2-T_4^2]r_P^{-2/5}-[T_2^2-(XT_4)^2]} \tag{22}$$

5.2. Weak gas degeneracy

For an ideal Fermi and Bose gas, under the higher temperature or lower-density condition, i.e., the condition of weak gas degeneracy, $0<z<1$, the Fermi integral $f_n(z)$ and the Bose integral $g_n(z)$ may be, respectively, expanded in power of z, i.e.,

$$\begin{cases}f_n(z)=\sum_{l=1}^{\infty}(-1)^{l-1}\frac{z^l}{l^n}\\ g_n(z)=\sum_{l=1}^{\infty}\frac{z^l}{l^n}\end{cases} \tag{23}$$

Consequently, the first approximation of the correction function can be expressed as [11,14]

$$F(T,P)=1\pm EP/T^{5/2} \tag{24}$$

where $E=(2\pi\hbar^2/m)^{3/2}/(4\sqrt{2}k^{5/2})$. By using Eq. (24), Eqs. (15) and (16) may be, respectively, simplified as

$$\begin{aligned}R={}&AU_LU_H(T_2-XT_4)(YT_2-T_4)\\&/\left\{U_H(YT_2-T_4)\ln\left[(T_L-XT_4)/(T_L-T_2)\right]\right.\\&\left.+U_L(T_2-XT_4)G\ln\left[(YT_2-T_H)/(T_4-T_H)\right]\right\}\end{aligned} \tag{25}$$

and

$$\varepsilon=\frac{1}{G-1} \tag{26}$$

where $G=\frac{(YT_2-T_4)\pm EP_H[1/(YT_2)^{3/2}-1/(T_4)^{3/2}]}{(T_2-XT_4)\pm EP_L[1/(T_2)^{3/2}-1/(XT_4)^{3/2}]}$.

5.3. At high temperatures

When the temperature of the gas is high enough and its density is low enough, the fugacity of the gas z is much smaller than unity and the correction function $F(T,P)=1$. The ideal Bose and Fermi gases become the ideal gas, and consequently, the quantum Brayton refrigeration cycle becomes the classical Brayton refrigeration cycle. In such a case, Eqs. (15) and (16) may be, respectively, simplified as [36]

$$\begin{aligned}R={}&AU_HU_L(T_2-XT_4)/\left\{U_H\ln\left[(T_L-XT_4)/(T_L-T_2)\right]\right.\\&\left.+U_L\ln\left[(YT_2-T_H)/(T_4-T_H)\right]\right\}\end{aligned} \tag{27}$$

and

$$\varepsilon=\frac{T_2-XT_4}{YT_2-T_4-T_2+XT_4} \tag{28}$$

Eqs. (27) and (28) have been used to analyze the performance of an irreversible Brayton refrigeration cycle and some significant results have been obtained [36].

5.4. Endoreversible cycle

When the irreversibility in the adiabatic processes is negligible, $\eta_c=\eta_e=1$ and $Y=1/X=r_P^{2/5}$. Because the value of $F(z)$ remains unchanged during a reversible isentropic

process [13], one can easily calculate $B = r_P^{2/5}$, and consequently, Eqs. (15) and (16) may be further simplified as

$$R = AU_H U_L\left(T_2 - r_P^{-2/5}T_4\right) / \left\{U_H \ln\left[(T_L - r_P^{-2/5}T_4)/(T_L - T_2)\right] + U_L \ln\left[(r_P^{2/5}T_2 - T_H)/(T_4 - T_H)\right]\right\} \tag{29}$$

and

$$\varepsilon = \frac{1}{r_P^{2/5} - 1} \tag{30}$$

It can be seen from Eqs. (29) and (30) that for an endoreversible quantum Brayton refrigeration cycle, the cooling rate is independent of the quantum degeneracy of the working substance and the coefficient of performance is only dependent on the pressure ratio.

It is significant to note that Eqs. (29) and (30) may be directly derived from Eqs. (27) and (28), respectively. It shows that the cooling rate and coefficient of performance of an endoreversible quantum Brayton refrigeration cycle are the same as those of an endoreversible Brayton refrigeration cycle using an ideal gas as the working substance. However, it should be pointed out that the refrigeration heat Q_L and the cycle period τ of an endoreversible quantum Brayton refrigeration cycle are different from those of an endoreversible Brayton refrigeration cycle using an ideal gas as the working substance. It is seen from Eqs. (8) and (10) that the refrigeration heat Q_L and the cycle period τ of an endoreversible quantum Brayton refrigeration cycle are still dependent on the quantum degeneracy of the working substance.

6. Discussion

It should be pointed out that like many other cryogenic refrigeration systems, regeneration is often adopted in the Brayton refrigeration cycle in order to improve the performance of the system. It may be clearly seen from the previous investigations of several authors that for an irreversible Brayton refrigeration cycle using the ideal gases as the working substances [23,36], the larger the rate of the regenerated heat is, the larger the cooling rate and coefficient of performance of the cycle. For an internal-irreversible Brayton refrigeration cycle working with the ideal Bose or Fermi gas [15,37], the refrigeration load and coefficient of performance of the cycle increase as the regenerative heat is increased. Using the Brayton refrigeration cycle model established here and the analysis method in Refs. [15,23–27,36,37], one can further discuss the performance of an irreversible regenerative Brayton refrigeration cycle working with the quantum gases.

7. Conclusions

The synthesis influence of the quantum degeneracy of the working substance, irreversibility of the adiabatic processes and finite-rate heat transfer between the working substance and the heat reservoirs on the performance characteristics of the Brayton refrigeration cycle working with an ideal quantum gas has been analyzed by using the theory of statistical mechanics. Expressions for several important parameters of the refrigeration cycle are derived and some curves, which can reveal the optimum performance characteristics of the cycle, are presented for a set of given parameters. The optimal regions of the coefficient of performance and power input are determined. Several interesting cases are discussed in detail. It can be clearly seen from these general expressions of important performance parameters and their corresponding curves that the performance characteristics of a Fermi or Bose Brayton cryogenic refrigeration cycle are different from those of a classical Brayton refrigeration cycle. The coefficient of performance and cooling rate are, in general, dependent not only on temperature and the thermal conductances between the working substance and the heat reservoirs but also on the pressure and other parameters, while the coefficient of performance of the classical Brayton cycle is only dependent on the ratio of pressure. It is also found that the influence of the pressure ratio, the irreversible adiabatic processes and the finite-rate heat transfer between the working substance and the heat reservoirs on the performance parameters of the cycle is remarkable. In addition, it is found from the characteristic curves that the optimal performance characteristics of the quantum Brayton refrigeration cycles using ideal Fermi or Bose gases as the working substance are different. Because of the influence of the quantum degeneracy, the coefficient of performance and cooling rate of the Fermi Brayton cryogenic refrigeration cycle are larger than those of the Bose Brayton cryogenic refrigeration cycle. The results obtained here will be helpful to the further understanding for the general optimum performance characteristics of quantum Brayton refrigeration cycles.

Acknowledgements

This work was supported by the National Natural Science Foundation (No. 10575084), People's Republic of China and the Science and Technology Program of Fujian's Education Department, People's Republic of China (No. JA06016).

References

[1] A. Sisman, H. Saygin, On the power cycles working with ideal quantum gases, J. Phys. D: Appl. Phys. 32 (1999) 664–670.
[2] H. Saygin, Quantum degeneracy, classical and finite-time thermodynamics: I. Basic concepts and some applications on efficiency analyses, in: Advances in Finite-Time Thermodynamics Conference, 12–14 November 2000, Jerusalem, Israel.
[3] H. Saygin, A. Sisman, Quantum degeneracy effect on the work output from a Stirling cycle, J. Appl. Phys. 90 (2001) 3086–3089.
[4] J. Chen, B. Lin, Low-temperature behavior of an ideal Bose gas and some forbidden thermodynamic cycles, J. Phys. A: Math. Gen. 36 (2003) 11385–11390.
[5] F. Wu, L. Chen, F. Sun, C. Wu, F. Guo, Optimization criteria for an irreversible quantum Brayton engine with an ideal Bose gas, J. Appl. Phys. 99 (2006) 054904.
[6] F. Wu, L. Chen, F. Sun, C. Wu, Q. Li, Generalized model and optimum performance of an irreversible quantum Brayton engine with spin systems, Phys. Rev. E 73 (2006) 016103.

[7] B. Lin, J. Chen, Performance analysis of irreversible quantum Stirling cryogenic refrigeration cycles and their parametric optimum criteria, Phys. Scr. 74 (2006) 251–258.
[8] H. Saygin, A. Sisman, Brayton refrigeration cycles working under quantum degeneracy conditions, Appl. Energy 69 (2001) 77–85.
[9] J. Chen, J. He, B. Hua, The inherent of regenerative losses on the performance of a Fermi Ericsson refrigeration cycle, J. Phys. A: Math. Gen. 35 (2002) 7995–8004.
[10] J. He, J. Chen, B. Hua, Influence of quantum degeneracy on the performance of a Stirling refrigerator working with an ideal Fermi gas, Appl. Energy 72 (2002) 541–554.
[11] Y. Zhang, B. Lin, J. Chen, The influence of quantum degeneracy and irreversibility on the performance of a Fermi quantum refrigeration cycle, J. Phys. A: Math. Gen. 37 (2004) 7465–7497.
[12] F. Wu, L. Chen, F. Sun, C. Wu, F. Guo, Optimal performance of an irreversible quantum Brayton refrigerator with ideal Bose gases, Phys. Scr. 73 (2006) 452–457.
[13] B. Lin, J. Chen, The performance analysis of a quantum Brayton refrigeration cycle with an ideal Bose gas, Open Sys. & Information Dyn. 10 (2003) 147–157.
[14] B. Lin, J. He, J. Chen, Quantum degeneracy effect on the performance of a Bose Ericsson refrigeration cycle, J. Non-Equilib. Thermodyn. 28 (2003) 221–232.
[15] Y. Yang, B. Lin, J. Chen, Influence of regeneration on the performance of a Brayton refrigeration-cycle working with an ideal Bose-gas, Appl. Energy 83 (2006) 99–112.
[16] J.M.M. Rocco, S. Velasco, A. Medina, A. Calvo Herandez, Optimum performance of a regenerative Brayton thermal cycle, J. Appl. Phys. 82 (1997) 2735–2741.
[17] L. Chen, C. Wu, F. Sun, Cooling load vs. COP characteristics for an irreversible air refrigeration cycle, Energy Convers. Mgmt. 39 (1998) 117–126.
[18] J. Luo, L. Chen, F. Sun, C. Wu, Optimum allocation of heat exchanger inventory of irreversible air refrigeration cycles, Phys. Scr. 65 (2002) 410–415.
[19] Y. Tu, L. Chen, F. Sun, C. Wu, Cooling load and coefficient of performance optimization for real air refrigerators, Appl. Energy 83 (2006) 1289–1306.
[20] S. Zhou, L. Chen, F. Sun, C. Wu, Cooling load density optimization of an irreversible simple Brayton refrigerator, Open Sys. & Information Dyn. 9 (2002) 325–337.
[21] L. Chen, S. Zhou, F. Sun, C. Wu, Performance optimization for an irreversible variable-temperature heat reservoir air refrigerator, Int. J. Ambient Energy 26 (2005) 180–190.
[22] C.K. Chen, Y.F. Su, Exergetic efficiency optimization for an irreversible Brayton refrigeration cycle, Int. J. Thermal Sci. 44 (2005) 303–310.
[23] L. Chen, S. Zhou, F. Sun, C. Wu, Performance of heat-transfer irreversible regenerated Brayton refrigerators, J. Phys. D: Appl. Phys. 34 (2001) 830–837.
[24] Y. Tu, L. Chen, F. Sun, C. Wu, Optimization of cooling load and COP for real regenerated air refrigerator, Proc. IMechE, Part E: J. Process Mech. Engrg. 220 (2006) 207–215.
[25] S. Zhou, L. Chen, F. Sun, C. Wu, Theoretical optimization of a regenerated air refrigerator, J. Phys. D: Appl. Phys. 36 (2003) 2304–2311.
[26] S. Zhou, L. Chen, F. Sun, C. Wu, Cooling-load density optimization for a regenerated air refrigerator, Appl. Energy 78 (2004) 315–328.
[27] S.K. Tyagi, G.M. Chen, Q. Wang, S.C. Kaushik, A new thermoeconomic approach and parametric study of an irreversible regenerative Brayton refrigeration cycle, Int. J. Refrigeration 29 (2006) 1167–1174.
[28] R.K. Pathria, Statistical Mechanics, second ed., Elsevier Press Ltd., Singapore, 1996.
[29] L.D. Landau, E.M. Lifshitz, Statistical Physics, Pergamon Press Ltd., London, 1958.
[30] C. Wu, L. Chen, F. Sun, Performance of a regenerative Brayton heat engine, Energy 21 (1996) 71–76.
[31] C.Y. Cheng, C.K. Chen, Power optimization of an endoreversible regenerative Brayton cycle, Energy 21 (1996) 241–247.
[32] A. Graziani, G. Dall'Oglio, L. Martinis, L. Pizzo, L. Sabbatini, A new generation of ^{3}He refrigerators, Cryogenics 43 (2003) 659–662.
[33] G.Q. Lu, P. Chen, On cycle-averaged pressure in a G-M type pulse tube refrigerator, Cryogenics 42 (2002) 287–293.
[34] M.J. Devlin, S.R. Dicker, J. Klein, M.P. Supanich, A high capacity completely closed-cycle 250 mK ^{3}He refrigeration system based on a pulse tube cooler, Cryogenics 44 (2004) 611–616.
[35] M.Y. Xu, A. de Waele, Y.L. Ju, A pulse tube refrigerator below 2 K, Cryogenics 39 (1999) 865–869.
[36] Y. Zhang, J. Chen, J. He, C. Wu, Comparison on the optimum performances of the irreversible Brayton refrigeration cycles with regeneration and non-regeneration, Appl. Thermal Engrg. 27 (2007) 401–407.
[37] Y. Zhang, B. Lin, J. Chen, The performance characteristics of an irreversible regenerative quantum refrigeration cycle, Phys. Scr. 73 (2006) 48–55.